# A Novel Process for Separation of Magnetite and Phosphorous Phases from a $CaO\text{-}SiO_2\text{-}FeO\text{-}P_2O_5$ slag

Guoxuan Li,[1)] Jinshan Liang,[1)] Jun Long,[1)] Dong Guan,[1)] Zushu Li,[2)] Seetharaman Sridhar[3)] and Juncheng Li[1)*]

1)School of materials science and Engineering, Jiangsu University, Zhenjiang 212013, China
2)WMG, The University of Warwick, Coventry, CV4 7AL UK
3)School for Engineering of Matter, Transport and Energy, Arizona State University Tempe, AZ 85287, USA

**Synopsis:**

Iron and phosphorus were successfully separated from $CaO$-$SiO_2$-$FeO$-$P_2O_5$ slag through atmospheric control, $B_2O_3$ addition and a combination of magnetic separation and flotation. For the slag with basicity ($CaO/SiO_2$) of 2.5 and $B_2O_3$ addition of 6% (weight percentage), iron and phosphorus in the slag were enriched in the form of magnetite ($Fe_3O_4$) and calcium phosphate ($Ca_{10}P_6O_{25}$) phases respectively under Ar atmosphere. Using a combination of magnetic separation and flotation, the concentrates were obtained with $Fe_3O_4$ and $P_2O_5$ content of 92.84 % and 37.66 % respectively, corresponding to the recovery ratios of 85.8 % for iron and 91.3 % for phosphorus.

**Keywords**: Steelmaking slag; $B_2O_3$ addition; Atmospheric control; Magnetite; Calcium phosphate

## 1. Introduction

Converter slag, a significant by-product during the steelmaking process, primarily contains CaO, $SiO_2$, $Fe_tO$ and $P_2O_5$, which are considered to be potential material sources for road construction,[1] cement,[1] fertilizer,[2] civil engineering projects[3] as well as feedstock for re-use in the steelmaking process. Re-use in the steel plant is limited by the enriched phosphate in steelmaking slags, since phosphorus may reverse to the hot metal. The $Fe_tO$, in the steelmaking slag is furthermore, a potential source for ferrous feedstock if it could be seperated. Various techniques such as flotation,[4] magnetic separation,[5] super gravity separation,[6-8] carbothermal reduction,[9] and selective leaching[10-12] have been employed to extract phosphorus from steelmaking slags. However, none of these approaches have achieved simultaneous recovery of both iron and phosphorus. A novel technology based on the principle of selective enrichment-selective growth-selective separation has been successfully applied to extract boron,[13] vanadium,[14] titanium from metallugical slags,[15] and many trials[16] have been carried out to selectively separate phosphorus from steelmaking slag. However, solid solution $2CaO{\cdot}SiO_2$-$3CaO{\cdot}P_2O_5$ ($C_2S$-$C_3P$) was the main phosphorus-enriched phase in steelmaking slag and the maximum content of $P_2O_5$ in $C_2S$-$C_3P$ was reported no more than 20%, particularly for the slag with basicity above 2.0.[17,18] Moreover, the abovementioned approaches primarily focused on extracting phosphorus from steelmaking slag, rather than simultaneously recycling iron and phosphorus as well as reusing tailings. Here, we present a successful method, based on the combination of magnetic separation and flotation methods, to selectively separate iron and phosphorus from $CaO$-$SiO_2$-$FeO$-$P_2O_5$ slag through atmospheric control and $B_2O_3$ addition.

## 2. Materials and methods

Based on the dephosphorization slag composition of the two converter steelmaking process (i.e. the first converter for dephosphorization and the second for decarburization), we synthesized the slag required for this study. The chemical composition of synthetic slags was presented in **Table 1**. As seen in the Table 1, the $P_2O_5$ content in all the slags were adjusted to 10 % and basicity ($CaO/SiO_2$) of the slags were kept at 2.5.

The powders of dry chemical agents were well mixed and then placed into a platinum crucible with diameter of 30 mm and height of 40 mm. The mixed powder (40 g for each slag) was heated in a

vertical tube furnace that was controlled by a program controller with U-type (Pt–30%Rh/Pt–6%Rh) thermocouple, within the observed precision range of ±3 °C. The experimental material was melted in the vertical tube furnace under air/argon gas atmosphere (with flow rate 0.5 L/min, 99.999%) at 1600 °C for 120 minutes to ensure it fully melted and then rapidly cooled to 900 °C at a cooling rate of 10 °C/min. Then the slags were water quenched and divided into two parts. One part was crushed by ball mill, and characterized by X-ray diffraction (TTRIII from Rigaku Corporation) and XRF (ARL Advant'X IntelliPower-4200) to obtain the respective mineral component and chemical composition, while the other part was characterized on the scanning electron microscopy (SEM), energy disperse spectrum (EDS; ZEISS EVO 18) and electron probe microanalysis (EPMA SHIMADZU 8050G) to obtain micromorphology and element distribution of the products. In order to separate phosphorus and iron phases from the quenched slags, a wet magnetic separator (XCGQ-500 from Hengcheng equipment Co., Ltd) with the magnetic field intensity of 3.0 KOe was firstly employed to separate magnetite phase from the quenched slags. The magnetic separation tube was located between the two ends of the C-type electromagnet and is equipped with a glass tube for reciprocating movement and swing. When the sorted sample passes through the magnetic field area, the magnetic part is attached near the tube wall, while the non-magnetic part is washed out by water during mechanical movement. Subsequently, the flotation machine (XFD-0.75L from Weiming equipment Co., Ltd) was used to separate phosphorus-enriched phase from the non-magnetic part of magnetic separation. The flotation machine is driven by the trigonometric generation of the motor to drive the impeller to rotate, resulting in centrifugal action to form negative pressure. On the one hand, the sufficient air is mixed with the slurry, and the slurry is mixed with the flotation reagent, including inhibitors, collectors and pH regulators. At the same time, the foam is refined, so that the mineral adheres to the foam and floats to the slurry surface to form a mineralized foam. Through adjusting the height of the gate and controlling the liquid level, the useful foam is scraped out by the scraper. During the flotation process, the pH value was controlled at 8.5-9 by adding sodium carbonate, the samples were roughened once and selected four times with water glass as inhibitor, oxidized paraffin soap and tall oil as mixed capture agent. In the process of roughing, sodium carbonate, water glass, oxidized paraffin soap and tall oil were 1500 g/t, 3000 g/t, 700 g/t and 500 g/t respectively. While for cleaning, sodium carbonate, water glass, oxidized paraffin soap and tall oil were 300 g/t, 500 g/t, 500 g/t and 300 g/t respectively (mixing for 3 min).

## 3. Results and discussion

The phases presented in the synthetic slags were characterized by XRD and the results are shown in **Fig. 1**. It can be seen that the main phases presented in the slag 1# were calcium ferrite ($Ca_2Fe_2O_5$), calcium silicate ($Ca_2SiO_4$) and phosphorus solid solution ($Ca_7Si_2P_2O_{16}$). This is in agreement with the experimental results[19,20] that wustite is inclined to oxidize to hematite under an air atmosphere and then stabilizes the free lime by forming brownmillerite ($Ca_2(Al, Fe)_2O_5$). However, with an atmosphere change from air to high purity argon, the main iron-containing phase ($Ca_2Fe_2O_5$) were found to change to the magnetite phase ($Fe_3O_4$), while other phases remain the same as the original slag. Furthermore, with the introduction of 6% $B_2O_3$ (slag 3#), the dicalcium silicate ($2CaO{\cdot}SiO_2$) and solid solution phase of $Ca_7Si_2P_2O_{16}$ were changed into $CaB_2O_4$, $CaFeSi_2O_6$ and phosphorus rich phase of calcium phosphate ($Ca_{10}P_6O_{25}$), while the magnetite phase remained the same. In summary, with the simultaneous atmospheric control and $B_2O_3$ addition into the simulated steelmaking slag, iron and phosphorus containing phases precipitated in the form of $Fe_3O_4$ and $Ca_{10}P_6O_{25}$ respectively during the cooling process from 1600 ºC to 900 ºC.

From the results of SEM-EDS analysis (**Fig. 2 and Table 1**), it is clear that the iron phase in the slags changed from irregular calcium ferrite ($Ca_2Fe_2O_5$) to regular spinel ($Fe_3O_4$), while the phosphorus phase in the slags transformed from slag matrix ($Ca_7Si_2P_2O_{16}$) to lath-shaped phase ($Ca_{10}P_6O_{26}$). In addition, the round granular dicalcium silicate phase ($2CaO{\cdot}SiO_2$) turned into slag matrix. The measured chemistry of the white spinel phase was close to $Fe_3O_{4.3}$, while the lath-shaped phase's chemistry was closest to $Ca_2P_{0.83}O_{3.51}$, corresponding to the $Fe_3O_4$ and $Ca_{10}P_6O_{25}$ phases in Fig. 1.

In order to quantitatively analyze the composition of various phases, slag 3# was analyzed using EPMA. The $P_2O_5$ content in the phosphorus enriched phase was detected to be 34.1%, which is almost twice as high as previous studies.[17,18] Moreover, the dominant composition of the spinel phase was $Fe_3O_4$ even through it was presented as $Fe_2O_3$ in **Table 3**. Therefore, in the whole paper, $Fe_2O_3$ content is converted to $Fe_3O_4$ based on the stoichiometry of $3Fe_2O_3 = 2Fe_3O_4 + O$.

In order to separate the abovementioned spinel ($Fe_3O_4$) and calcium phosphate ($Ca_{10}P_6O_{25}$) phases from modified slags, a combination of magnetic separation and flotation separation were carried out. The XRD results of the concentrates and tailings obtained by magnetic separation and flotation

separation are shown in **Fig. 4**. It can be seen that magnetic separation can separate the treated slag into two parts: the concentrates of magnetite $Fe_3O_4$ and the mixture (remaining slag) of $CaB_2O_4$, $CaFeSi_2O_6$ and $Ca_{10}P_6O_{25}$. After applying the flotation separation, the remaining slag from magnetic separation can be split into concentrates $Ca_{10}P_6O_{25}$ and tailings (primarily $CaB_2O_4$ and $CaFeSi_2O_6$).

The products obtained in different stages were tested by XRF, the results were shown in **Table 4**. $Fe_3O_4$ in the concentrate of magnetic separation was 92.84%, $P_2O_5$ content in the concentrate after floatation separation was 37.66%, and $P_2O_5$ contents in the tailing was 1.95%.

The recovery ratios of Fe and P in the concentrates and tailings can be calculated by Eqs. (1) and (2):

$$\varepsilon_{Fe}=\frac{m_{c1}\times\omega_{Fe1}}{m_{c1}\times\omega_{Fe1}+m_{c2}\times\omega_{Fe2}+m_r\times\omega_{Fe3}}\times 100\text{pct} \quad (1)$$

$$\varepsilon_{P}=\frac{m_{c2}\times\omega_{P2}}{m_{c1}\times\omega_{P1}+m_{c2}\times\omega_{P2}+m_r\times\omega_{P3}}\times 100\text{pct} \quad (2)$$

where $\varepsilon_{Fe}$ and $\varepsilon_{P}$ are the recovery ratios of Fe and P in the slag, pct; $m_{c1}$, $m_{c2}$ and $m_r$ are the mass of magnetic separation concentrate, flotation concentrate and flotation tailings respectively, pct; $\omega_{Fe1}$, $\omega_{Fe2}$, $\omega_{Fe3}$ and $\omega_{P1}$, $\omega_{P2}$, $\omega_{P3}$ are the mass fraction of Fe and P in magnetic separation concentrate, flotation concentrate and flotation tailings, pct. As shown in Table 4, the recovery ratio of iron and phosphorus were 85.8 % and 91.3 %.

Based on the investigation results in this study, it is possible to separate iron and phosphorus enriched phases from steelmaking slag as well as comprehensively utilize the steelmaking slag as illustrated in **Fig. 5**, and further investigation will focus on the enriching mechanism of iron and phosphorus phases in the slags with atmospheric control and $B_2O_3$ addition.

## 4. Conclusion

In summary, it was confirmed by the experimental result that iron and phosphorus could be effectively recoved from $CaO\text{-}SiO_2\text{-}FeO\text{-}P_2O_5$ through atmospheric control and $B_2O_3$ addition. Using a combination of magnetic separation and flotation separation, the concentrates were obtained with the $Fe_3O_4$ and $P_2O_5$ content of 92.84 % and 37.66 % respectively, corresponding to the recovery ratios of 85.8 % for iron and 91.3 % for phosphorus. The results suggest the current approach to be a potential method for the comprehensive utilization of basic oxygen steelmaking slag.

## Acknowledgement

This work was supported by Jiangsu University (19JDG011). J LI would like to acknowledge the support from innovation training program for undergraduate (202010299076 and 202110299463X) and scientific research projects (18A001, 18A003,18A014 and 20A007).

# Reference


1) J. Li, C. Luo, M. Sun, W. Shen, B. Cao and X. Li: *Key Eng. Mater*., **3019**(2014)**,** 9. http://doi.org/10.4028/www.scientific.net/KEM.599.98.

2) L. Lin, Y. Liu, J. Zhi, S. He, X. Li, Z. Hou and L. Zhang: *Ironmak. Steelmak*., **48**(2021), 334. http://doi.org/10.1080/03019233.2020.1780366.

3) S. Israel, T. Carlos, A. P. Juan, S. Jesus and T. Pablo: *Appl. Sci*., **10**(2020), 773. http://doi.org/10.3390/app10030773.

4) Z. Wang, B. Liang and J. Zhang: *Appl. Mech. Mater.*, **522**(2014), 1501. http://doi.org/10.4028/www.scientific.net/AMM.

5) K. Matsubae-Yokoyama, H. Kubo and T. Nagasaka: *IJSJ Int*., **50**(2010), 65. http://doi.org/10.2355/isijinternational.

6) X. Lan, J. Gao, Y. Du and Z. Guo: *J. Alloys Compd*., **731**(2018), 873.http://doi.org/10.1016/j.jallcom.2017.10.100.

7) J. Gao, Y. Li, G. Xu and Z. Guo: *ISIJ Int*., **57**(2017), 587. http://doi.org/10.2355/isijinternational.ISIJINT-2016-601.

8) J. Gao, L. Guo, Y. Zhong, H. Ren and Z. Guo: *Int. J. Miner., Metall. Mater*., **23**(2016), 743. http://doi.org/CNKI:SUN:BJKY.0.2016-07-002.

9) Y. Zhang, Q. Xue, G. Wang and J. Wang: *ISIJ Int*., **58**(2018), 2219. http://doi.org/10.2355/isijinternational.ISIJINT-2018-372.

10) S. Sugiyama, I. Shinomiya, R. Kitora and M. Katoh: *J. Chem. Eng. Jpn*., **47**(2014), 483. http://doi.org/10.1252/jcej.13we065.

11) M. Numata, N. Maruoka, S.-J. Kim and S. Y. Kitamura: *ISIJ Int.*, **54**(2014), 1983.http://doi.org/10.2355/isijinternational.54.1983.

12) C. Du, X. Gao, S.-J. Kim and S. Y. Kitamura: *ISIJ Int.*, **56**(2016), 1436. https://doi.org/10.2355/isijinternational.ISIJINT-2016-022

13) X. Yang, H. Matsuura and F. Tsukihashi: *ISIJ Int*., **49**(2009), 1298. http://doi.org/10.2355/isijinternational.49.1298.

14) S. Liu, L. Wang and K. Chou: *Waste Manage*., **127**(2021), 179. http://doi.org/10.1016/J.WASMAN.2021.04.034.

15) H. Fan, R. Wang, Z. Xu, H. Duan and D. Chen: *Crystals*.,**8**(2021), 888. http://doi.org/10.3390/CRYST11080888.

16) B. Zhu, M. Zhu, J. Luo, X. Qiu, Y. Wang, Q. Zhang and B. Xie: *Metals*., **8**(2021), 1160. http://doi.org/10.3390/MET11081160.

17) J. Li, M. Zhang, M. Guo and X. Yang: *Int. J. Miner., Metall. Mater*., **5**(2016), 520. http://doi.org/CNKI:SUN:BJKY.0.2016-05-004.

18) J. Li, M. Zhang, M. Guo and X. Yang: *Metall. Mater. Trans. B*., **45**(2014), 1666. http://doi.org/10.1007/s11663-014-0085-0.

19) C. Liu, S. Huang, B. Bart and M. Guo: *Metall. Mater. Trans. B*., **50**(2019), 210. http://doi.org/10.1007/s11663-018-1444-z.

20) C. Liu, M. Guo, L. Pandelaers, B. Blanpain and S. Huang: *Metall. Mater. Trans. B*., **47**(2016), 3237. http://doi.org/10.1007/s11663-016-0809-4.

**Table captions:**

Table 1 Composition and oxygen partial pressure of simulated steel slag；

Table 2 EDS analysis data of the composition of the samples before and after modification；

Table 3 EPMA analysis data of the composition of slag 3#；

Table 4 XRF results of products and recovery ratio of P and Fe in the slag

179 Table 1 Composition and oxygen partial pressure of simulated steel slag

| Slag No | Composition(mass%) | | | | | Atmosphere |
|---|---|---|---|---|---|---|
| | CaO | $SiO_2$ | FeO | $P_2O_5$ | $B_2O_3$ | |
| 1 | 38.57 | 15.34 | 36 | 10 | 0 | Air |
| 2 | 38.57 | 15.34 | 36 | 10 | 0 | Ar |
| 3 | 34.29 | 13.71 | 36 | 10 | 6 | Ar |

180

181

182 Table 2 EDS analysis data of the composition of the samples before and after modification

| Slag No. | Position | Phases | Ca(at.%) | Si(at.%) | O(at.%) | P(at.%) | Fe(at.%) | Potential Formula |
|---|---|---|---|---|---|---|---|---|
| 1 | Pt1 | Fe-rich | 20.61 | 5 | 20.66 | - | 53.73 | $Ca_2Fe_{3.7}O_{4.8}$ |
| | Pt2 | Matrix | 50.9 | 16.32 | 31.67 | - | 1.02 | $Ca_2Si_{0.91}O_{3.1}$ |
| | Pt3 | P-rich | 43.26 | 20.06 | 22.33 | 14.35 | - | $Ca_7Si_{4.67}P_{2.98}O_{9.1}$ |
| 2 | Pt4 | Fe-rich | 3.32 | - | 26.35 | - | 70.33 | $Fe_3O_{3.93}$ |
| | Pt5 | Matrix | 50.04 | 15.9 | 33.61 | - | 0.45 | $Ca_2Si_{0.91}O_{3.4}$ |
| | Pt6 | P-rich | 44.82 | 19.77 | 23.06 | 12.35 | - | $Ca_7Si_{4.44}P_{2.15}O_{11}$ |
| 3 | Pt7 | Fe-rich | - | - | 29.11 | - | 70.89 | $Fe_3O_{4.3}$ |
| | Pt8 | Matrix | 41.78 | 16.98 | 27.5 | 1.34 | 12.4 | $CaFe_{0.21}Si_{0.58}O_{1.64}$ |
| | Pt9 | P-rich | 49.37 | 0.06 | 34.55 | 16.02 | - | $Ca_2P_{0.83}O_{3.51}$ |

-The amount of the phase is below the lower detection limit.

The X-ray energy of element B is very low which is hard to detect, so B is not listed in Table 2.

183

184

185 Table 3 EPMA analysis data of the composition of slag 3#

| Spots | Phases | Composition(mass%) | | | | | |
|---|---|---|---|---|---|---|---|
| | | CaO | $SiO_2$ | "$Fe_2O_3$" | $P_2O_5$ | $B_2O_3$ | Total |
| 1 | P-rich | 51.79 | 5.407 | 0.97 | 34.1 | 3.66 | 95.95 |
| 2 | Matrix | 40.21 | 25.37 | 13.38 | 1.612 | 11.9 | 92.48 |
| 3 | Fe-rich | 0.5 | 0.02 | 99.19 | 0 | 0 | 99.7 |

The measured composition of iron is reported as $Fe_2O_3$ for presentation purposes.

186

187

188 Table 4 XRF results of products and recovery ratio of P and Fe in the slag

| Products | Mass(g) | Composition(mass%) | | | | | Recovery ratio(Pct) | |
|---|---|---|---|---|---|---|---|---|
| | | CaO | $SiO_2$ | $P_2O_5$ | $Fe_2O_3$ | Corresponding $Fe_3O_4$ | P | Fe |
| Concentrate(magnetic) | 14.2 | 3.2 | 1.3 | 0.46 | 96.04 | 92.84 | 1.55 | 85.8 |
| Concentrate(flotation) | 10.2 | 59.8 | 1.74 | 37.66 | 0.8 | 0.72 | 91.3 | 0.475 |
| Tailing(flotation) | 15.6 | 48.26 | 35.78 | 1.95 | 14.01 | 13.54 | 7.13 | 13.73 |

189
190

**Figure captions：**

Figure 1 XRD analysis of samples；

Figure 2 SEM morphology of samples: (a) 1#; (b) 2#; (c) 3#；

Figure 3 EPMA image characterization of slag 3#；

Figure 4 XRD patterns of the phase after separation；

Figure 5 Flow sheet of comprehensively utilization of steelmaking slag

Figure 1

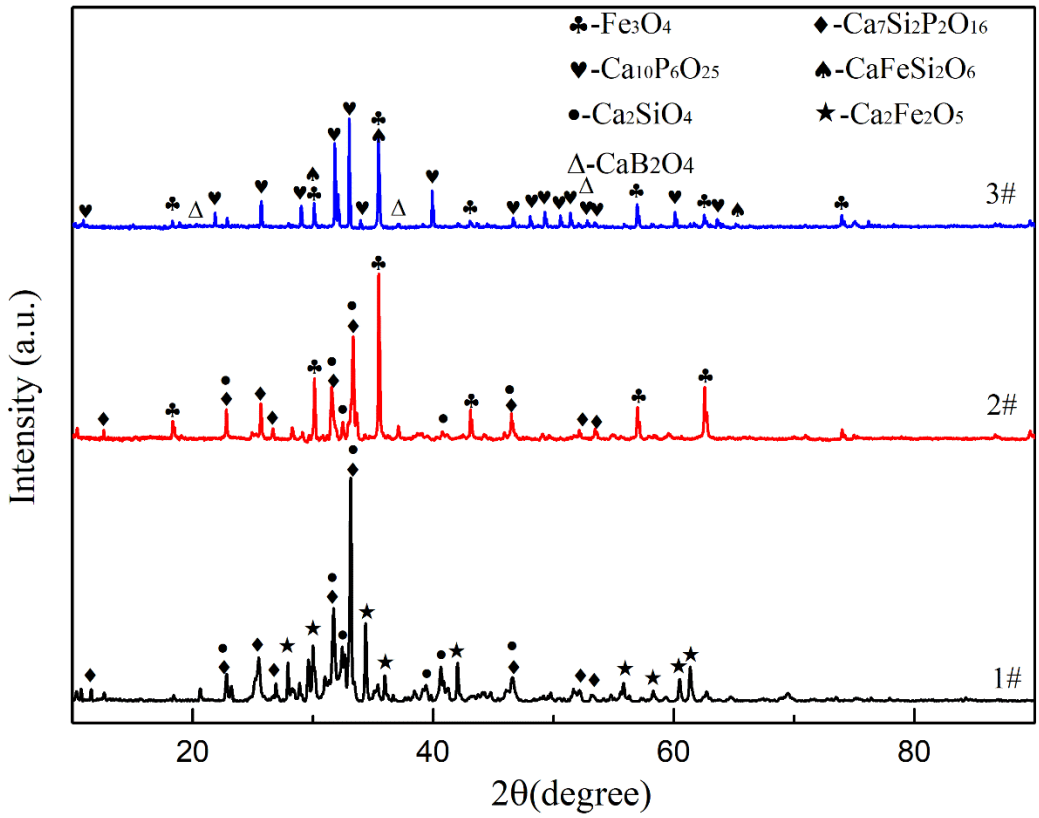
♣-Fe3O4
♦-Ca7Si2P2O16
♥-Ca10P6O25
♠-CaFeSi2O6
●-Ca2SiO4
★-Ca2Fe2O5
Δ-CaB2O4
3#
2#
1#
Intensity (a.u.)
20
40
60
80
2θ(degree)

Figure 2

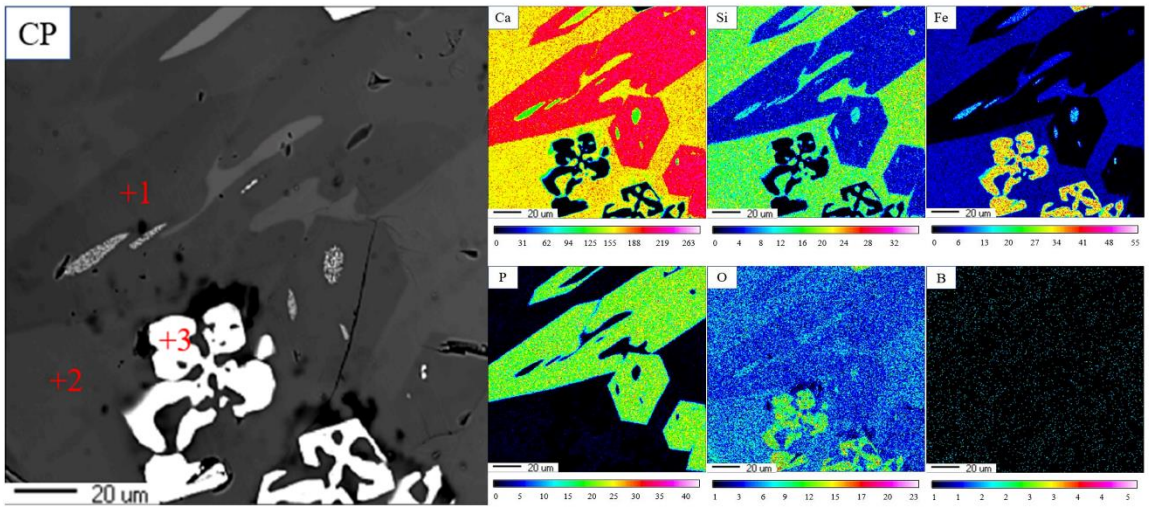

Figure 3

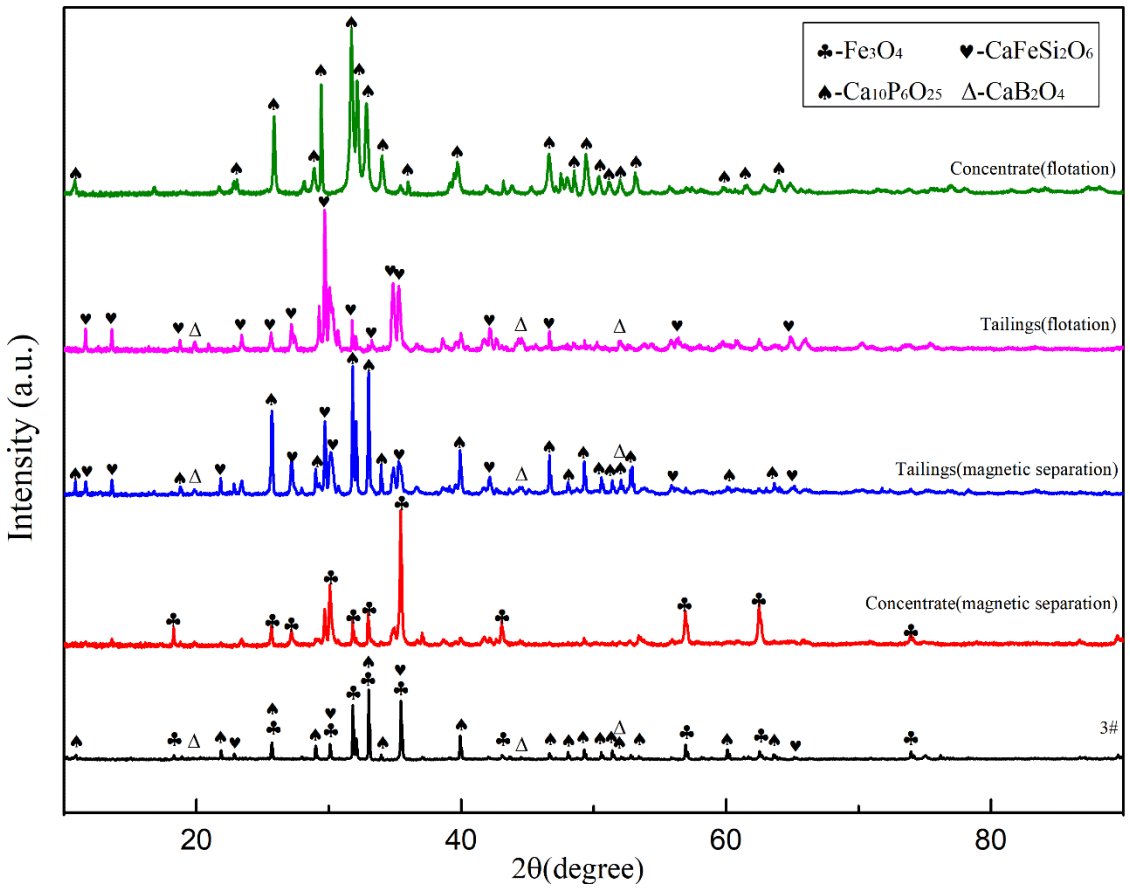
♣-Fe3O4
♥-CaFeSi2O6
♠-Ca10P6O25
Δ-CaB2O4
Concentrate(flotation)
Tailings(flotation)
Tailings(magnetic separation)
Concentrate(magnetic separation)
3#
Intensity (a.u.)
20
40
60
80
2θ(degree)

Figure 4

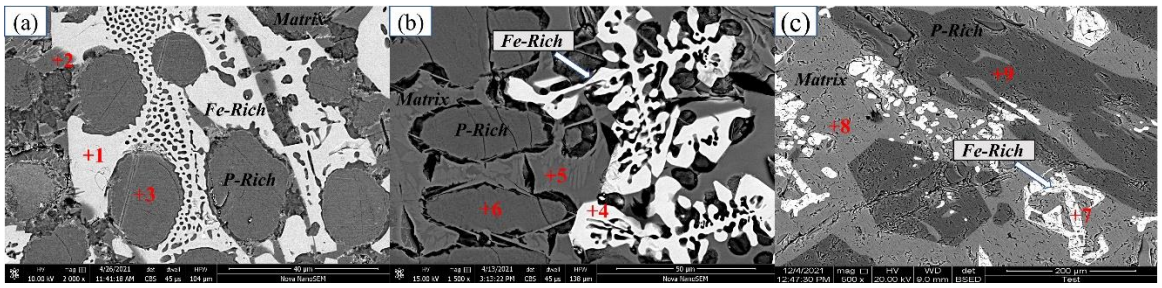
(a)
Matrix
+2
Fe-Rich
+1
+3
P-Rich
(b)
Fe-Rich
Matrix
P-Rich
+5
+6
+4
(c)
P-Rich
Matrix
+9
+8
Fe-Rich
+7

301 Figure 5

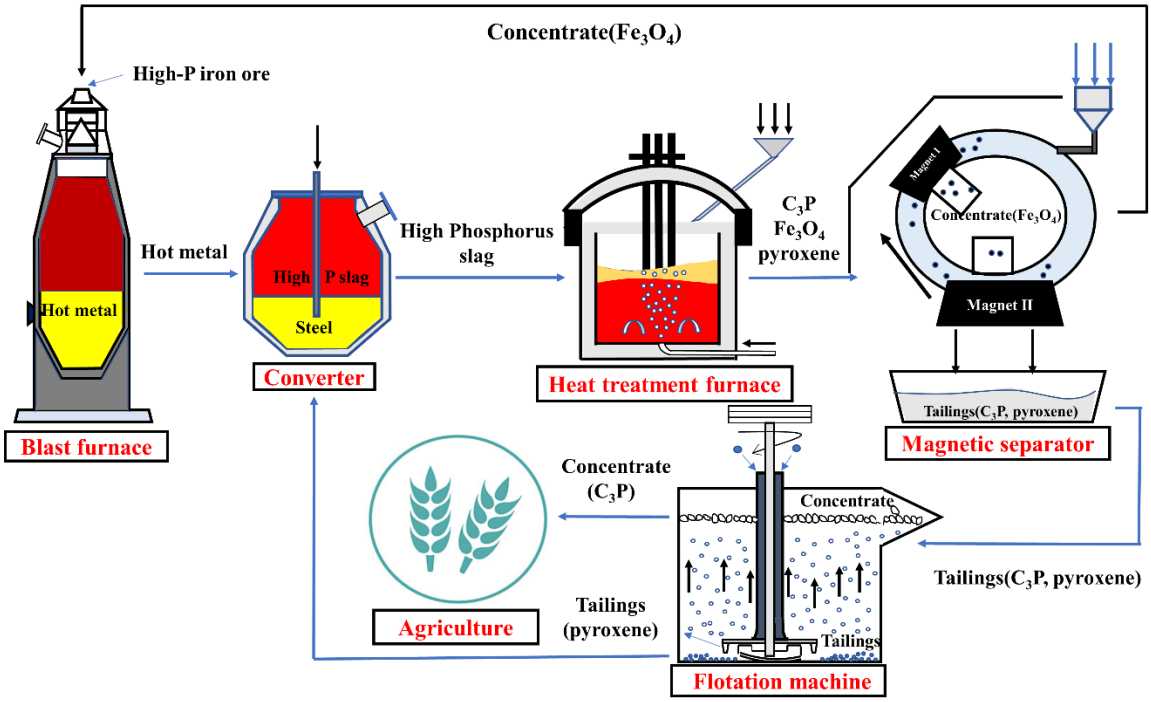


302